



25 **Abstract**

26 **Background:** The 15q13.3 microdeletion has pleiotropic effects ranging from  
27 apparently healthy to severely affected individuals. The underlying basis of the variable  
28 phenotype remains elusive.

29 **Methods:** We analyzed gene expression using blood from 3 individuals with 15q13.3  
30 microdeletion and brain cortex tissue from 10 mice Df[h15q13]/+. We assessed differentially  
31 expressed genes (DEGs), protein-protein interaction (PPI) functional modules, and gene  
32 expression in brain developmental stages.

33 **Results:** The deleted genes' haploinsufficiency was not transcriptionally compensated,  
34 suggesting a dosage effect may contribute to the pathomechanism. DEGs shared between  
35 tested individuals and a corresponding mouse model show a significant overlap including  
36 genes involved in monogenic neurodevelopmental disorders. Yet, network-wide  
37 dysregulatory effects suggest the phenotype is not caused by a singular critical gene. A  
38 significant proportion of blood DEGs, silenced in adult brain, have maximum expression  
39 during the prenatal brain development. Based on DEGs and their PPI partners we identified  
40 altered functional modules related to developmental processes, including nervous system  
41 development.

42 **Conclusions:** We show that the 15q13.3 microdeletion has a ubiquitous impact on the  
43 transcriptome pattern, especially dysregulation of genes involved in brain development. The  
44 high phenotypic variability seen in 15q13.3 microdeletion could stem from an increased  
45 vulnerability during brain development, instead of a specific pathomechanism.

46 **Keywords:** 15q13.3; Copy number variants; Transcriptomics; Protein-protein  
47 interaction networks; Nervous System Development.

## 48 **Introduction**

49 Individuals with 15q13.3 microdeletion (OMIM #612001) show clinical  
50 manifestations ranging from no obvious symptoms to severe intellectual disability,  
51 neuropsychiatric disorders, and epilepsy<sup>1</sup> (Fig. 1 A, B). The most common 15q13.3 deletion  
52 spans 2 Mb and includes eight RefSeq genes (*CHRNA7*, *FAN1*, *TRPM1*, *KLF13*, *OTUD7A*,  
53 *MTMR10*, *ARHGAP11B*, and *MIR211*, Fig. 1A)<sup>2</sup>. Many functional and association studies  
54 inquired which gene(s) encompassed by the deleted region could be responsible for the  
55 phenotype. However, the results were as variable as the clinical manifestation and different  
56 groups proposed multiple candidates (*CHRNA7*<sup>3,4</sup>, *OTUD7A*<sup>5,6</sup>, *FAN1*<sup>7</sup>, *ARHGAP11B*<sup>8</sup>,  
57 *TRPM1*<sup>9</sup>, *KLF13*<sup>10</sup>), to explain the symptoms (Fig. 1A). A mouse model of the 15q13.3  
58 microdeletion syndrome (Df[h15q13]/+) shows manifestations similar to affected humans  
59 ranging from attention deficits to impaired behavior and disrupted prefrontal cortex  
60 processing<sup>11</sup>. Thus, the microdeletion effect is stable across species and clearly impairs  
61 nervous system function.

62 Recently, it was suggested that many disrupted biological pathways such as Wnt  
63 signaling or ribosome biogenesis may be involved in the molecular mechanism underlying the  
64 disease rather than singular dosage-affected genes<sup>12</sup>. While Zhang *et al.* used a multiomics  
65 approach to identify perturbed biological processes, the multiple employed analyses showed  
66 disagreement with respect to the pathomechanism. Also, no shared dysregulated genes were  
67 identified between human induced pluripotent stem cells (iPSCs) and mouse cortex<sup>12</sup>. This  
68 could be a result of the *in vitro* setup and neuronal differentiation protocols, which generally  
69 impact gene expression profiles<sup>13</sup>. We thus sought to inquire gene expression profiles in  
70 subjects with 15q13.3 microdeletion in a native/*in vivo* state.

71 One major challenge of transcriptomics in a clinical setting is tissue-specific gene  
72 expression<sup>14,15</sup> and the fact that most of the times the only accessible tissue to probe is blood  
73<sup>16</sup>. In our previous work we showed, however, that known genes for neurodevelopmental  
74 disorders are not necessarily expressed in the adult brain and that genes which are relevant  
75 during embryonic development of the central nervous system can be silenced at a later  
76 timepoint<sup>14</sup>. Thus, although not regarded as a representative tissue, blood transcriptomics has  
77 the potential to reveal aspects missed in other tissues or iPSCs.

78 In the present study, we analyzed the changes in gene expression profiles in the blood  
79 of three individuals with heterozygous microdeletion 15q13.3 and intellectual disability  
80 associated with epilepsy. We identified a significant overlap ( $p$ -value = 0.02) of 68

81 differentially expressed genes (DEGs) between humans and mouse (*Df[h15q13]/+*) cortex.  
82 The gene ontology (GO) category most significantly enriched with DEGs was “nervous  
83 system development–GO:0007399” and DEGs in blood, which are not expressed in the adult  
84 brain, revealed maximum expression levels in the prenatal stage of brain development. The  
85 disrupted gene expression profile could lead to an increased vulnerability in the early stages  
86 of nervous system development.

## 87 **Materials and Methods**

### 88 *Ethics approval*

89 This study was approved and monitored by the ethics committee of the University of  
90 Leipzig, Germany (224/16-ek and 402/16-ek).

### 91 *Chr15q13.2q13.3 microdeletion individuals and mouse model (Df[h15q13]/+)*

92 Three individuals with diagnosed heterozygous 15q13.2q13.3 microdeletions were  
93 previously described<sup>17</sup>. For all individuals we performed Illumina TruSight One Panel and  
94 microarray analysis. Patient 1 is a male with a deletion of 2.56 Mbp  
95 (15q13.2q13.3(30366247\_32927476)x1). The second patient is female and carries a deletion  
96 on chromosome 15 of 1.57 Mbp (15q13.2q13.3(30936285\_32514341)x1). Patient 3 is a male,  
97 has a deletion of 2.14 Mbp on chromosome 15 (15q13.2q13.3(30371774\_32514341)x1). He  
98 was additionally diagnosed with a maternally inherited splicing-variant in the remaining  
99 *TRPM1* allele and a heterozygous *de novo* point mutation in *MITF*. Pathogenic variants in  
100 *MITF* gene cause albinism, which was also clinically diagnosed in this individual. His  
101 ophthalmological phenotype (severe myopia, astigmatism, and pendular nystagmus) were  
102 clinical symptoms of the autosomal recessive *TRPM1* phenotype (one allele being deleted as  
103 part of the 15q13.3 microdeletion and the other allele carrying the maternally inherited  
104 splicing variant). In sum, he suffered from a complex combined phenotype with neurologic  
105 symptoms attributed to the 15q13.3 microdeletion. Blood RNA samples were taken from the  
106 three individuals (two males and one female, aged 27–63 years) and four control subjects  
107 (two males and two females, aged 20–52 years).

108 To identify molecular changes which are consistent across species we used the data  
109 generated by Gordon and colleagues (GSE129891)<sup>18</sup>. We analyzed transcriptomes from  
110 cerebral cortex tissue of mice with heterozygous deletions on mouse chromosome 7qC  
111 syntenic to human 15q13.3<sup>11,18</sup>.

## 112 ***RNA extraction and sequencing***

113 RNA was extracted from PAXgene blood samples using PAXgene Blood RNA Kit  
114 (Qiagen). RNA sequencing (RNA-seq) libraries were prepared using TruSeq RNA Library  
115 Prep Kit v2 (Illumina, San Diego, CA) and sequenced on an Illumina NovaSeq platform with  
116 151 bp paired-end reads.

## 117 ***Differential Gene Expression (DEG) analysis***

118 RNA-seq reads were mapped to the human genome assembly hg38 with STAR  
119 (version 2.6.1d)<sup>19</sup>. We computed the transcript levels with htseq-count (version 0.6.0)<sup>20</sup>.  
120 From GSE129891 we analyzed read counts of ten wild type and ten (Df[h15q13]/+) mouse  
121 cerebral cortex samples. Genes with a sum of less than 10 reads in all samples together were  
122 excluded from further analysis. Differential expression of genes was determined with the R  
123 package DESeq2 (version 1.30.1)<sup>21</sup>, which uses the Benjamini-Hochberg method to correct  
124 for multiple testing<sup>22</sup>. Genes were considered to be significantly differentially expressed if  $p$ -  
125 adj < 0.05. To check clustering of RNA-sequencing samples of subjects and controls, a  
126 principal component analysis (PCA) was performed with the R package pcaExplorer (version  
127 2.6.0)<sup>23</sup>. RNA count data were variance stabilized transformed and the 500 most variant  
128 genes (top n genes) were selected for computing the principal components.

## 129 ***Expression of DEGs in different developmental stages***

130 Expression data of DEGs were obtained from PTEE (version 1.1)<sup>14</sup> for the adult brain  
131 cortex. Genes expressed at a low level in adult brain tissue may be expressed at a higher level  
132 in the developing brain and therefore, could still play a significant role in neurodevelopment.  
133 Hence, for DEGs expressed <1.5 TPM in adult brain cortex (according to PTEE), expression  
134 levels in different developmental stages were obtained from the R package ABAEnrichment  
135 (version 1.20.0)<sup>24</sup> for the whole brain. We used a Tukey's HSD test to determine whether this  
136 group of DEGs (<1.5 TPM in adult brain cortex) displays a significantly different expression  
137 profile between the brain developmental stages.

138 DEGs which are expressed <1.5 TPM in adult brain cortex but >1.5 RPKM in prenatal  
139 stage of the whole brain and reach their maximum of expression in the prenatal stage were  
140 selected and further analyzed for GO enrichment.

141 ***DEGs involved in NDDs***

142 A list of genes, which are known to play a role in NDDs, was obtained from PTEE<sup>14</sup>.  
143 DEGs of 15q13.2q13.3 microdeletion patients were compared to the list of NDD genes, to  
144 determine DEGs that could contribute to the neurological symptoms observed in those  
145 patients. The significance for enrichment of DEGs with NDD genes was calculated using a  
146 binomial test in R<sup>25</sup>.

147 ***GO enrichment***

148 Gene ontology enrichment analysis was performed with the R package GOfuncR  
149 (version 1.14.0) for up- and down-regulated DEGs<sup>26</sup>. GO nodes with a family wise error rate  
150 (FWER) <0.05 were considered significantly enriched. To check for unspecific GO  
151 enrichment analysis results, the four control subjects were split in two groups and differential  
152 gene expression and GO enrichment analyses were performed for those two control groups.

153 ***Identification of activated/inactivated DEG-interacted functional modules***

154 We investigated the activity of DEG-interacted functional modules to elucidate the  
155 roles of DEGs in 15q microdeletion. The DEG-interacted network was constructed by the  
156 DEGs and their interacting partners in the human protein interaction network (PIN), which  
157 was obtained from the InBio Map database<sup>27</sup>. A DEG-interacted functional module is a  
158 subnetwork of the DEG-interacted network formed by genes annotated by the same biological  
159 processes. The functional annotations of genes were obtained from GO<sup>28,29</sup>, and only the  
160 annotations supported by experiments were used in this study. Additionally, to ensure the  
161 DEGs' participation and functional association among genes, all the functional modules were  
162 required to contain at least one DEG and one interaction. To determine if the member genes  
163 of the tested functional module were overrepresented at the top of the entire ranked gene list,  
164 we performed the gene set enrichment analysis (GSEA)<sup>30</sup> for evaluating each module's  
165 activity and inactivity separately. To assess the activity (inactivity), the entire gene list was  
166 ranked downward (upward) by the fold change of genes between the 15q microdeletion and  
167 controls. We then calculated the enrichment score (ES) for each functional module by  
168 walking down the ranked gene list. The ES of functional module  $f$  is defined as below:

$$ES_f = \max(S_i), i \in \{1, \dots, N\}$$
$$S_i = \sum_{j=0}^i p \times \frac{1}{N_f} - (1-p) \times \frac{1}{(N-N_f)}, \text{ where } p = \begin{cases} 0 \\ 1, \text{ if gene } i \in f \end{cases}$$

169 where  $S_i$  is the score of gene  $i$ ,  $i$  is ordered by fold change,  $N_f$  is the number of genes in  
170 the tested functional module,  $N$  is the number of total ranked genes, and  $p$  is a binary  
171 parameter. To estimate the significance of  $ES_f$ , we produced 1,000 scores  $ES_{rand}$  calculated  
172 from 1,000 randomly permuted gene lists. Then, we denoted the standard score  $z$ , which was  
173 defined as below, as the activity or inactivity of functional module  $f$ .

$$z = \frac{ES_f - \mu}{\sigma}$$

174 where  $\mu$  and  $\sigma$  are respectively the mean and standard deviation of 1,000  $ES_{rand}$ .  
175 Finally, the functional modules possessing  $z$  of activity greater than two and  $z$  of inactivity  
176 less than zero were defined as activated; and the functional modules with  $z$  of inactivity  
177 greater than two and  $z$  of activity less than zero were defined as inactivated. The discovered  
178 activated or inactivated functional modules were further summarized/clustered by the  
179 REVIGO<sup>31</sup> algorithm with similarity  $\geq 0.9$  that was calculated from Resnik<sup>32</sup> algorithm and  
180 visualized using the treemap package<sup>33</sup>.

181 To predict key transcription factors and cofactors that drive transcriptomic differences  
182 between microdeletion individuals and controls we used Mining Algorithm for GenetIc  
183 Controllers (MAGIC), which leverages ENCODE ChIP-seq data to look for statistical  
184 enrichment of transcription factors and cofactors in genes and flanking regions<sup>34</sup>.

## 185 **Results**

### 186 *Transcriptional changes in 15q13.3 microdeletion individuals and Df[h15q13]/+ mice*

187 To study the effects of the 15q13.3 microdeletion on transcriptional regulation, we  
188 performed RNA-seq from three individuals carrying a heterozygous 15q13.3 microdeletion  
189 (Fig. 1) and four control subjects. Further, to identify robust changes across species and  
190 tissues, we analyzed cerebral cortex tissue from ten mice (Df[h15q13]/+) reported by Gordon  
191 *et al.*<sup>18</sup>. While in the 15q13.3 microdeletion subjects we identified 2,334 genes (adjusted *p*-  
192 value < 0.05) with altered expression levels compared to controls (Supplementary Table S1),  
193 only genes within the deleted region withstood multiple testing correction in the mouse  
194 (Supplementary Table S1). This could be related to a difference in synteny between the  
195 mouse and human chromosomal regions, to the high interindividual variability of our  
196 subjects, or to the generally mild impact on gene expression with genes not reaching the  
197 dysregulation threshold necessary to withstand conservative multiple testing correction. The  
198 immediate result of applying multiple testing correction is that the probability a true effect  
199 may be rejected will increase<sup>35</sup>. To control for false positives, but also to avoid erroneously  
200 rejecting real effects we decided to focus on DEGs shared between human and mouse. We,  
201 thus, considered genes with uncorrected *p*-value < 0.05 in the mouse and identified 68 shared  
202 genes between the two species and different tissues (Supplementary Table S1). To test  
203 whether the number of overlapping genes is higher than expected by chance we performed  
204 100,000 random samplings considering a total of 20,000 genes. This yielded a *p*-value of 0.02  
205 suggesting the overlap is significant. By contrast, when we considered DEGs among controls,  
206 only six genes were shared with the (Df[h15q13]/+) mouse model, which is an amount  
207 expected to occur by chance (*p*-value=0.94 from 100,000 simulations).

208 To check whether the gene dosage affects gene expression, we identified genes located  
209 in the deleted site, which are expressed in blood and brain cortex (Supplementary Fig. S1).  
210 Four genes have an expression higher than 1.5 TPMs in brain cortex<sup>14</sup> (*FANI*, *MTMR10*,  
211 *KLF13*, *OTUD7A*) of which *MTMR10* and *KLF13* are also highly expressed in blood  
212 (Supplementary Fig. S1). These genes were significantly downregulated in both human and  
213 mouse samples (Supplementary Table S1). Moreover, although *FANI* and *OTUD7A* display  
214 low expression levels in blood (Supplementary Fig. S1), they were also significantly  
215 differentially expressed in our blood transcriptome analysis (Supplementary Table S1).

216 We next focused on shared DEGs between 15q13.3 microdeletion individuals and the  
217 mouse model. Variants in eight of these genes (*PHIP*, *KAT6A*, *VPS13B*, *GPAA1*, *CHD7*,



218 *FIBP, KMT2C, AP1S1*) are known causes for monogenic NDD<sup>36</sup>. There are six genes which  
219 have a gene ontology (GO) annotation related to gene expression (*ZFP57, EDA, KAT6A,*  
220 *CD46, PIK3R3*) and also six genes related to brain development (*CHD7, ITGA4, MYLIP,*  
221 *PAFAH1B3, SIRT2, B4GALT2*). Interestingly, we could also identify components of the  
222 major histocompatibility complex, class II to be dysregulated in both blood and brain  
223 (Supplementary Table S1), which may reflect a disturbed inflammatory or immune process.

#### 224 ***Molecular pathways affected by transcriptome alterations in 15q13.3 microdeletion***

225 To identify molecular pathways that may be affected by the gene expression profiles  
226 we performed GO enrichment analysis followed by protein-protein-interaction (PPI)  
227 networks, as previously described<sup>37,38</sup>. Using the mouse data, we identified general GO  
228 categories like cellular components or developmental processes to be enriched with DEGs  
229 (Supplementary Table S2). For human subjects, there were two less general GO terms which  
230 were most significantly enriched with DEGs: “nervous system development” (GO:0007399,  
231 *p*-value after family wise error rate (FWER) multiple correction = 0.036) with 32 associated  
232 genes and “DNA binding” (GO:0003677, *p*-value FWER multiple correction = 0.046) with  
233 183 associated genes (Table 1, Supplementary Table S2).

234 To better delineate molecular pathways, involved in the copy-number variant (CNV)  
235 pathomechanism, we further focused on identifying the functional modules formed by DEGs  
236 from human subjects and their PPI partners. This revealed that most nodes clustered in  
237 cellular processes like metabolic pathways, signaling, or cellular components (Fig. 2,  
238 Supplementary Table S2). Since regulation of gene expression appeared to be perturbed, we  
239 tested if the gene expression profile matches dysregulation of one or more transcription  
240 factors based on ENCODE Chip-seq data<sup>34</sup>. This analysis revealed no significant enrichment  
241 for genes associated with a known transcription regulator, suggesting that a single gene  
242 cannot explain the observed expression profile. Interestingly, inactivated functional modules  
243 clusters are mainly involved in immune response and regulation of gene expression (Fig. 2B,  
244 Supplementary Table S2). Oligodendrocyte differentiation and development appear to be  
245 affected, which together with the “positive regulation of neuron death” (Fig. 2A, B,  
246 Supplementary Table S2) could explain the impaired nervous system development. To check  
247 whether those molecular pathways are specifically identified in the microdeletion individuals,  
248 we analyzed differential gene expression between two control groups. GO terms significantly  
249 enriched with DEGs of the control groups were mostly related to immune response, and to a  
250 much lesser extent to gene expression regulation (Supplementary Table S2). Thus, the

251 identification of those molecular pathways in the individuals bearing 15q13.3 microdeletion  
252 may not be related to the deleted region, but rather to the analyzed tissue. In contrast, we did  
253 not identify any GO terms related to nervous system development in the controls. This  
254 supports our hypothesis that the effect on pathways related to nervous system development in  
255 the affected individuals is a result of the microdeletion.

256 We showed that affected genes were enriched in pathways related to nervous system  
257 development (Table 1) and that PPIs influence apoptosis and neuron death (Fig. 2B). This  
258 prompted us to inquire all DEGs that have known Mendelian associations with monogenic  
259 NDD. We identified 252 of the DEGs to be related to monogenic intellectual disability (Fig.  
260 2C, Supplementary Table S1). The number of genes is significantly higher than expected by  
261 chance ( $p$ -value binomial test = 0.003), which could suggest an underlying polygenic effect  
262 that leads to an increased risk for a neurodevelopmental disorder.

### 263 *Dysregulated genes in 15q13.3 microdeletion individuals expressed in the developing brain*

264 Further, we asked whether blood DEGs, which are not expressed in the adult brain  
265 cortex, may have been expressed in the developing brain. We identified 358 DEGs, which are  
266 expressed in blood but not in the adult brain. We used the ABAEnrichment package in R<sup>24</sup> to  
267 check the expression levels of these genes during the different stages of brain development  
268 (Supplementary Table S3). For 245 of the 358 genes, we could retrieve expression levels from  
269 the Allen Brain Atlas. Our analysis revealed that for DEGs, which are silenced in the adult  
270 brain, there is a significant enrichment for the ones with a maximum expression level in the  
271 developing brain ( $p$ -value = 0.04, Fig. 3). A GO enrichment analysis of the 53 genes showed  
272 that several of these genes are involved in chromosome organization during cell division, but  
273 also identified the e.g. *DRAXIN* gene to be dysregulated, which is involved in the  
274 development of spinal cord (Supplementary Table S3).

### 275 **Discussion**

276 The 15q13.3 microdeletion is associated with pleiotropic effects and has been  
277 described in a wide spectrum of clinical contexts ranging from apparently healthy individuals  
278 to some severely affected with ID, epilepsy or even schizophrenia (Fig. 1B)<sup>2</sup>. It is difficult to  
279 dissect the mechanisms contributing to the nervous system developmental disturbance mostly  
280 because of the limitations of *in vitro* approaches aiming to reproduce human brain  
281 development<sup>10</sup>. Thus, the etiology of the 15q13.3 microdeletion's range of hypervariable  
282 symptoms remains elusive.

283 To understand how dysregulation of gene expression contributes to 15q13.3  
284 microdeletion pathomechanisms, we aimed to circumvent artefacts introduced by  
285 conventional *in vitro* approaches. Thus, we analyzed transcriptional profiles from three  
286 individuals with 15q13.3 microdeletion in an *in vivo* state in blood, which is an easily  
287 accessible tissue. To identify genes, which are robustly dysregulated we additionally analyzed  
288 brain cortex tissue from a 15q13.3 microdeletion mouse model.

289 We initially checked for dosage effects of the genes included in the microdeletion  
290 (Fig. 1A). This revealed that there are four genes with high expression in brain cortex  
291 (Supplementary Fig. S1<sup>14</sup>): *FANI*, *MTMR10*, *KLF13*, *OTUD7A*, all of which showed  
292 significant down-regulation in blood (Supplementary Table S1) of our subjects, as well as  
293 mouse brain cortex, confirming that a gene dosage effect of the microdeletion contributes to  
294 the transcriptional dysregulation. Other genes included in the typical deletion region: *TRPM1*,  
295 *CHRNA7*, *MIR211*, *ARHGAP11B*, display low expression levels in brain cortex and blood  
296 (Supplementary Fig. S1) and were not significantly differentially expressed in the 15q13.3  
297 microdeletion individuals. While *MIR211* is a microRNA, which was not sequenced probably  
298 as a result of the library preparation protocol and *ARHGAP11B* is a human specific gene<sup>36</sup>,  
299 *Trpm1* and *Chrna7* were down-regulated in mouse brain cortex (Supplementary Table S1),  
300 further supporting the importance of the haploinsufficiency.

301 We next focused on dysregulated genes across the two different tissues in the human  
302 subjects and the mouse model. One of the shared down-regulated genes is *CHD7*, which is  
303 frequently associated with CHARGE syndrome and has been shown to be highly relevant for  
304 neuronal differentiation and brain development<sup>39</sup>. *CDH7*, but also other shared dysregulated  
305 genes like *KMT2C* and *KAT6A* are involved in chromatin remodeling and hence in regulation  
306 of gene expression. This is in accordance with the findings of Zhang *et al.*, who described a  
307 global epigenomic reprogramming of iPSCs from 15q13.3 microdeletion individuals<sup>12</sup>.  
308 However, in their approach they were not able to identify driving factors, potentially  
309 secondary to the bias induced by *in vitro* cultivation. This could also explain why they do not  
310 identify any shared dysregulations with the mouse model and their multiomics approach  
311 yielded a rather low correlation level among the multiple analyses.

312 To identify affected molecular pathways we performed a GO analysis of DEGs. This  
313 showed a significant enrichment of DEGs that are involved in DNA binding (Table 1).  
314 Moreover, an analysis of functional modules formed by DEGs and their PPI partners  
315 confirmed that gene expression regulation is affected (Fig. 2B, Supplementary Table 2). Yet,

316 based on ENCODE data<sup>34</sup>, we did not identify any transcription factor that could explain the  
317 observed transcriptional profile. This is in accordance with the observation of Zhang *et al.*  
318 that the disease-relevant impact of the 15q13.3 microdeletion is probably caused by the  
319 combinatorial effects of several genes, rather than a single “master” gene. Our analysis  
320 showed network-wide dysregulatory effects and explains why knockout models of singular  
321 genes encompassed in the deletion could not fully recapitulate the phenotype<sup>3-10</sup>.

322 The GO analysis also revealed that DEGs show a significant enrichment in the  
323 nervous system development category (Table 1). Indeed, we could show that the set of  
324 dysregulated genes contained a significant proportion ( $p$ -value = 0.003) of genes which have  
325 been related to monogenic NDD (Fig. 2C, Supplementary Table S1). The PPI functional  
326 module analysis identified more specific developmental processes of the nervous system like  
327 oligodendrocyte differentiation, axon and neuron projection development, as well as “positive  
328 regulation of neuron death” to be affected (Fig. 2A, B, Supplementary Table S2). This aligns  
329 with experimental data from Df[h15q13]/+ mice, which shows that both loss of *OTUD7A* and  
330 *CHRNA7* contribute to dendrite outgrowth defects<sup>3,6</sup>, and also with the recently described  
331 involvement of *Klf13* in the development of cortical interneurons.<sup>10</sup>

332 To determine whether other DEGs silenced in the adult human brain might have  
333 played a role in the nervous system development, we used the Allen Brain Atlas data, which  
334 provides brain gene expression data during different developmental stages.<sup>24</sup> This showed  
335 that a significant number of genes found to be differentially expressed in blood, but silenced  
336 in the adult brain had maximum expression levels in the prenatal stage (Fig. 3).

337 Our data suggests that network-wide dysregulatory effects contribute to 15q13.3  
338 microdeletion pathomechanisms. There are several lines of evidence that indicate a disturbed  
339 nervous system development, suggesting the severity of 15q13.3 microdeletion individuals’  
340 symptoms is probably determined in the early embryonic stages. The identification of  
341 dysregulated genes clustering in inflammatory and immune pathways may be related to the  
342 analyzed tissue, namely blood. However, since we identified components of the major  
343 histocompatibility complex, class II to be dysregulated in the mouse brain, we cannot rule out  
344 that immune insults could contribute to the increased vulnerability of 15q13.3 microdeletion-  
345 bearing offspring.

346 A major limitation of our study is the small cohort, in which individual-characteristic  
347 gene expression levels, which were not caused by the microdeletion, can have a big impact on  
348 the analysis. We attempted to circumvent this by comparing our data to the mouse model.

349 However, a larger cohort and potentially the analysis of an additional tissue like skin, could  
350 further refine the analysis and unveil which gene network is mostly responsible for the  
351 pathomechanism. This is crucial for directing future efforts to minimize the severity of the  
352 phenotype.

### 353 **Acknowledgements**

354 We are grateful that our patients and their families agreed to participate in this study.  
355 We thank Sandra Schinkel, Kathleen Lehmann, and Sophie Behrendt for their great technical  
356 assistance and Rigo Schulz for server support. We are grateful to Torsten Schöneberg for his  
357 input and help to draw Fig. 1.

### 358 **Author contributions**

359 MK performed gene expression analyses, contributed to the design of the study and  
360 writing of the manuscript. AV and LB supported bioinformatic analyses and performed GO  
361 enrichment analyses. MR performed wet lab work and contributed to the design of the study.  
362 CCL performed PPI analyses and contributed to manuscript writing. PZ recruited patients,  
363 performed phenotyping, and coordinated the genetic diagnosis. TB, AT, KP, and JH  
364 performed genetic diagnosis and contributed to the writing of the manuscript. AK, AM, NS,  
365 TL, KP, JRL, and AG contributed to analysis design, data interpretation, and writing of the  
366 manuscript. RAJ and DLD designed the study, coordinated the contact to patients, contributed  
367 to genetic diagnosis, gene expression analysis, and writing of the manuscript.

### 368 **Funding**

369 This study is funded by the Else Kröner-Fresenius-Stiftung 2020\_EKEA.42 to DLD  
370 and the German Research Foundation SFB 1052 project B10 to DLD and AG. DLD is funded  
371 through the “Clinician Scientist Programm, Medizinische Fakultät der Universität Leipzig”.  
372 Open Access funding enabled and organized by Projekt DEAL.

### 373 **Data availability**

374 RNA sequencing reads and expression profiles have been submitted to the Gene  
375 Expression Omnibus (<http://www.ncbi.nlm.nih.gov/geo/>) under accession number  
376 GSE197903. The code used for analyzing data has been deposited under  
377 <https://github.com/akhilvelluva/15q13.3>.

378

379

## 380 **References**

- 381 1. van Bon, B. W., Mefford, H. C. & de Vries, B. B. *15q13.3 Microdeletion*.  
382 *GeneReviews*® (University of Washington, Seattle, 2015).
- 383 2. Lowther, C., Costain, G., Stavropoulos, D. J., Melvin, R., *et al.* Delineating the  
384 15q13.3 microdeletion phenotype: A case series and comprehensive review of the  
385 literature. *Genetics in Medicine* vol. 17 149–157 (2015).
- 386 3. Gillentine, M. A., Yin, J., Bajic, A., Zhang, P., *et al.* Functional Consequences of  
387 CHRNA7 Copy-Number Alterations in Induced Pluripotent Stem Cells and Neural  
388 Progenitor Cells. *Am. J. Hum. Genet.* **101**, 874–887 (2017).
- 389 4. Hoppman-Chaney, N., Wain, K., Seger, P. R., Superneau, D. W., *et al.* Identification of  
390 single gene deletions at 15q13.3: Further evidence that CHRNA7 causes the 15q13.3  
391 microdeletion syndrome phenotype. *Clin. Genet.* **83**, 345–351 (2013).
- 392 5. Yin, J., Chen, W., Chao, E. S., Soriano, S., *et al.* Otud7a Knockout Mice Recapitulate  
393 Many Neurological Features of 15q13.3 Microdeletion Syndrome. *Am. J. Hum. Genet.*  
394 **102**, 296–308 (2018).
- 395 6. Uddin, M., Unda, B. K., Kwan, V., Holzapfel, N. T., *et al.* OTUD7A Regulates  
396 Neurodevelopmental Phenotypes in the 15q13.3 Microdeletion Syndrome. *Am. J. Hum.*  
397 *Genet.* **102**, 278–295 (2018).
- 398 7. Ionita-Laza, I., Xu, B., Makarov, V., Buxbaum, J. D., *et al.* Scan statistic-based  
399 analysis of exome sequencing data identifies FAN1 at 15q13.3 as a susceptibility gene  
400 for schizophrenia and autism. *Proc. Natl. Acad. Sci. U. S. A.* **111**, 343–348 (2014).
- 401 8. Florio, M., Albert, M., Taverna, E., Namba, T., *et al.* Human-specific gene  
402 ARHGAP11B promotes basal progenitor amplification and neocortex expansion.  
403 *Science (80-. )*. **347**, 1465–1470 (2015).
- 404 9. Hori, T., Ikuta, S., Hattori, S., Takao, K., *et al.* Mice with mutations in *Trpm1*, a gene  
405 in the locus of 15q13.3 microdeletion syndrome, display pronounced hyperactivity and  
406 decreased anxiety-like behavior. *Mol. Brain* **14**, 1–16 (2021).
- 407 10. Malwade, S., Gasthaus, J., Bellardita, C., Andelic, M., *et al.* Identification of  
408 Vulnerable Interneuron Subtypes in 15q13.3 Microdeletion Syndrome Using Single-  
409 Cell Transcriptomics. *Biol. Psychiatry* (2021) doi:10.1016/j.biopsych.2021.09.012.

- 410 11. Nilsson, S. R. O., Celada, P., Fejgin, K., Thelin, J., *et al.* A mouse model of the  
411 15q13.3 microdeletion syndrome shows prefrontal neurophysiological dysfunctions  
412 and attentional impairment. *Psychopharmacology (Berl)*. **233**, 2151–2163 (2016).
- 413 12. Zhang, S., Zhang, X., Purmann, C., Ma, S., *et al.* Network Effects of the 15q13.3  
414 Microdeletion on the Transcriptome and Epigenome in Human-Induced Neurons. *Biol.*  
415 *Psychiatry* **89**, 497–509 (2021).
- 416 13. Solomon, E., Davis-Anderson, K., Hovde, B., Micheva-Viteva, S., *et al.* Global  
417 transcriptome profile of the developmental principles of in vitro iPSC-to-motor neuron  
418 differentiation. *BMC Mol. Cell Biol.* **22**, (2021).
- 419 14. Velluva, A., Radtke, M., Horn, S., Popp, B., *et al.* Phenotype-tissue expression and  
420 exploration (PTEE) resource facilitates the choice of tissue for RNA-seq-based clinical  
421 genetics studies. *BMC Genomics* **22**, 802 (2021).
- 422 15. Frésard, L., Smail, C., Ferraro, N. M., Teran, N. A., *et al.* Identification of rare-disease  
423 genes using blood transcriptome sequencing and large control cohorts. *Nat. Med.* **25**,  
424 911–919 (2019).
- 425 16. Curry, P. D. K., Broda, K. L. & Carroll, C. J. The Role of RNA-Sequencing as a New  
426 Genetic Diagnosis Tool. *Curr. Genet. Med. Rep.* **9**, 13–21 (2021).
- 427 17. Zacher, P., Mayer, T., Brandhoff, F., Bartolomaeus, T., *et al.* The genetic landscape of  
428 intellectual disability and epilepsy in adults and the elderly: a systematic genetic work-  
429 up of 150 individuals. *Genet. Med.* **23**, 1492–1497 (2021).
- 430 18. Gordon, A., Forsingdal, A., Klewe, I. V., Nielsen, J., *et al.* Transcriptomic networks  
431 implicate neuronal energetic abnormalities in three mouse models harboring autism and  
432 schizophrenia-associated mutations. *Mol. Psychiatry* **26**, 1520–1534 (2021).
- 433 19. Dobin, A., Davis, C. A., Schlesinger, F., Drenkow, J., *et al.* STAR: Ultrafast universal  
434 RNA-seq aligner. *Bioinformatics* **29**, 15–21 (2013).
- 435 20. Anders, S., Pyl, P. T. & Huber, W. HTSeq-A Python framework to work with high-  
436 throughput sequencing data. *Bioinformatics* **31**, 166–169 (2015).
- 437 21. Love, M. I., Huber, W. & Anders, S. Moderated estimation of fold change and  
438 dispersion for RNA-seq data with DESeq2. *Genome Biol.* **15**, (2014).
- 439 22. Benjamini, Y., Drai, D., Elmer, G., Kafkafi, N., *et al.* Controlling the false discovery  
440 rate in behavior genetics research. in *Behavioural Brain Research* vol. 125 279–284

- 441 (Behav Brain Res, 2001).
- 442 23. Marini, F. & Binder, H. PcaExplorer: An R/Bioconductor package for interacting with  
443 RNA-seq principal components. *BMC Bioinformatics* **20**, (2019).
- 444 24. Grote, S., Prüfer, K., Kelso, J. & Dannemann, M. ABAEnrichment: An R package to  
445 test for gene set expression enrichment in the adult and developing human brain.  
446 *Bioinformatics* **32**, 3201–3203 (2016).
- 447 25. Team, R. C. R: A language and environment for statistical computing. (2013).
- 448 26. Grote, S. GOfuncR: Gene ontology enrichment using FUNC. *R Packag. version 1.5.1*  
449 (2018).
- 450 27. Li, T., Wernersson, R., Hansen, R. B., Horn, H., *et al.* A scored human protein-protein  
451 interaction network to catalyze genomic interpretation. *Nat. Methods* **14**, 61–64 (2016).
- 452 28. Ashburner, M., Ball, C. A., Blake, J. A., Botstein, D., *et al.* Gene ontology: Tool for  
453 the unification of biology. *Nature Genetics* vol. 25 25–29 (2000).
- 454 29. Carbon, S., Douglass, E., Dunn, N., Good, B., *et al.* The Gene Ontology Resource: 20  
455 years and still GOing strong. *Nucleic Acids Res.* **47**, D330–D338 (2019).
- 456 30. Subramanian, A., Tamayo, P., Mootha, V. K., Mukherjee, S., *et al.* Gene set  
457 enrichment analysis: A knowledge-based approach for interpreting genome-wide  
458 expression profiles. *Proc. Natl. Acad. Sci. U. S. A.* **102**, 15545–15550 (2005).
- 459 31. Supek, F., Bošnjak, M., Škunca, N. & Šmuc, T. Revigo summarizes and visualizes  
460 long lists of gene ontology terms. *PLoS One* **6**, (2011).
- 461 32. Resnik, P. Semantic Similarity in a Taxonomy: An Information-Based Measure and its  
462 Application to Problems of Ambiguity in Natural Language. *J. Artif. Intell. Res.* **11**,  
463 95–130 (1999).
- 464 33. Tennekes, M. Package ‘treemap’ Type Package Title Treemap Visualization. (2021).
- 465 34. Roopra, A. MAgIC: A tool for predicting transcription factors and cofactors driving  
466 gene sets using ENCODE data. *PLoS Comput. Biol.* **16**, e1007800 (2020).
- 467 35. Groenwold, R. H. H., Goeman, J. J. & Le Cessie, S. Multiple testing: When is many  
468 too much? *Eur. J. Endocrinol.* **184**, E11–E14 (2021).
- 469 36. Xing, L., Kubik, Zahorodna, A., Namba, T., Pinson, A., *et al.* Expression of  
470 human-specific ARHGAP11B in mice leads to neocortex expansion and increased



- 471 memory flexibility. *EMBO J.* **40**, (2021).
- 472 37. Jäger, E., Schulz, A., Lede, V., Lin, C.-C., *et al.* Dendritic Cells Regulate GPR34  
473 through Mitogenic Signals and Undergo Apoptosis in Its Absence. *J. Immunol.* **196**,  
474 2504–2513 (2016).
- 475 38. Le Duc, D., Lin, C. C., Popkova, Y., Yang, Z., *et al.* Reduced lipolysis in lipoma  
476 phenocopies lipid accumulation in obesity. *Int. J. Obes.* **45**, 565–576 (2021).
- 477 39. Feng, W., Kawachi, D., Körkel-Qu, H., Deng, H., *et al.* Chd7 is indispensable for  
478 mammalian brain development through activation of a neuronal differentiation  
479 programme. *Nat. Commun.* **8**, 1–14 (2017).
- 480 40. Karczewski, K. J., Francioli, L. C., Tiao, G., Cummings, B. B., *et al.* The mutational  
481 constraint spectrum quantified from variation in 141,456 humans. *Nature* **581**, 434–443  
482 (2020).

483

484

## 485 **Figure legends**

486 **Fig. 1.** Overview of the 15q13.3 locus and symptoms associated with the  
487 microdeletion A. Schematic representation of the 15q13.3 microdeletion region. Protein  
488 coding genes within the region are shown beneath chromosome 15. The color legend  
489 corresponds to the pLI score as a measure of loss-of-function deleteriousness<sup>40</sup>. Underlined  
490 genes have been considered candidates that are responsible for the observed phenotypes  
491 (*CHRNA7*<sup>3,4</sup>, *OTUD7A*<sup>5,6</sup>, *FANI*<sup>7</sup>, *ARHGAP11B*<sup>8</sup>, *TRPM1*<sup>9</sup>, *KLF13*<sup>10</sup>) B. Individuals with  
492 15q13.3 microdeletion display a heterogenous phenotype which can range from normal  
493 development to severe intellectual disability (ID) or neurodevelopmental disorders (NDD). A  
494 delineation of the phenotype based on 246 cases revealed predominantly neurologic  
495 symptoms of which ID, epilepsy, and neuropsychiatric disorders are most prominent<sup>2</sup>.

496 **Fig. 2.** Functional modules representation. A. Activated functional modules clusters in  
497 individuals with 15q13.3 microdeletion. Functions that could influence nervous system  
498 development are clustered in oligodendrocyte differentiation under the “cellular  
499 differentiation” category. The size of the boxes is proportional to the activation level of the  
500 module. B. Inactivated functional modules clusters in individuals with 15q13.3 microdeletion.  
501 These include processes relevant for neuron development. The size of the boxes is

502 proportional to the inactivation level of the module. C. 252 of the DEGs are related to  
503 monogenic neurodevelopmental disorders (NDD). The number of genes is significantly  
504 higher than expected by chance ( $p$ -value binomial test = 0.003).

505 **Fig. 3.** Inquiry of DEGs which are not expressed in the adult brain cortex. Based on  
506 the Allen Brain Atlas these genes show a significant enrichment for genes with highest  
507 expression level in the prenatal stage ( $p$ -value adult vs. prenatal stage = 0.04).

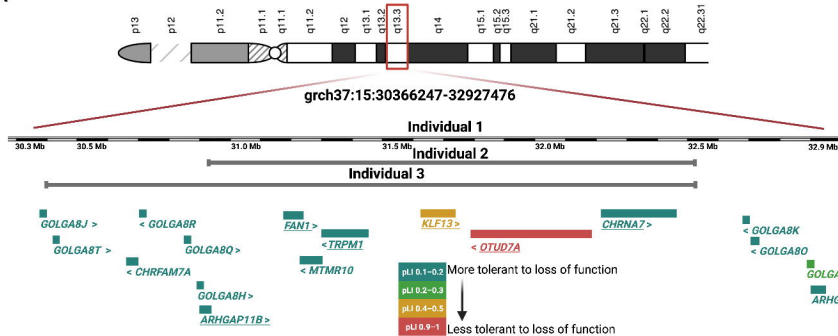
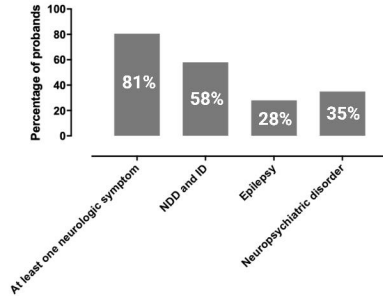
508

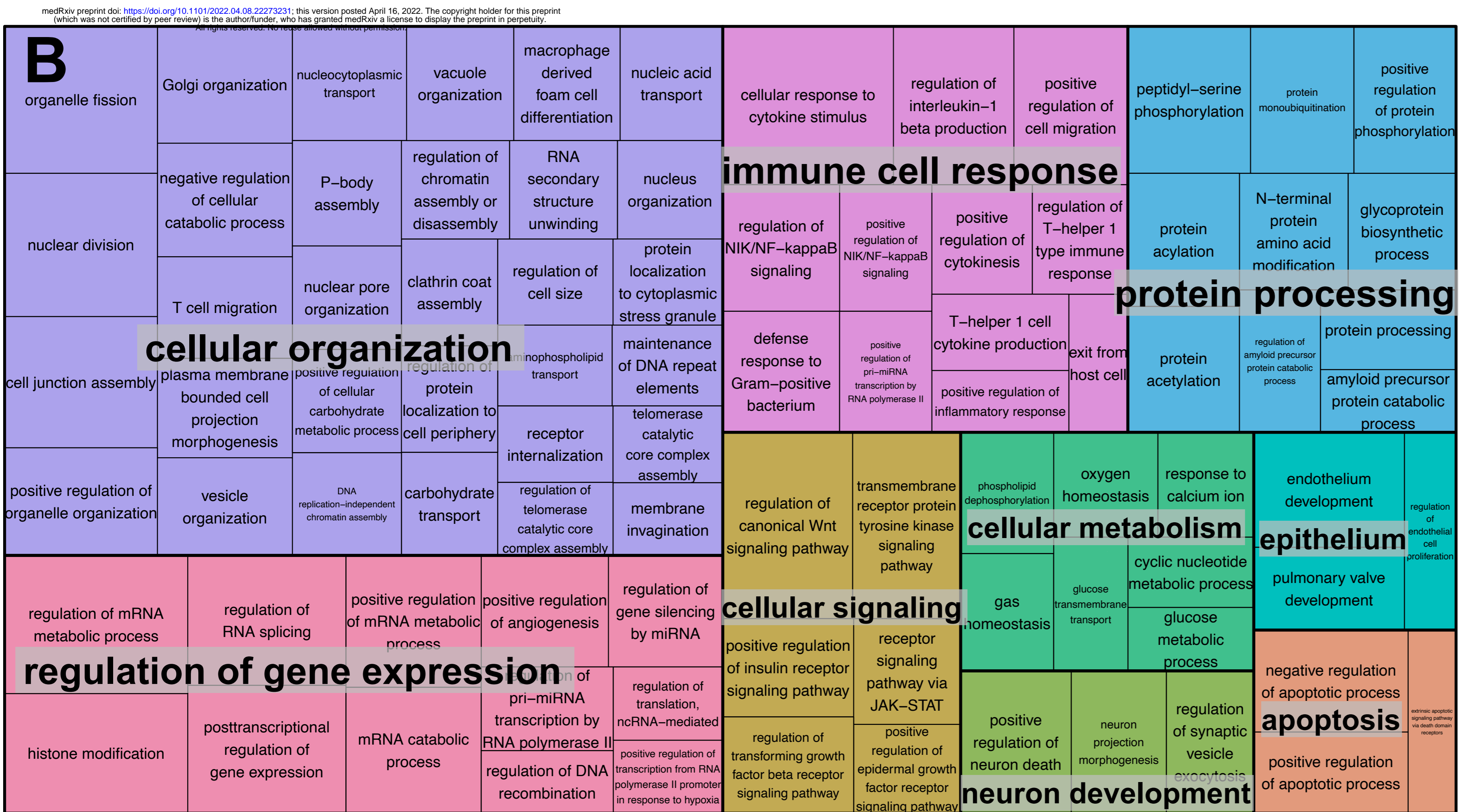
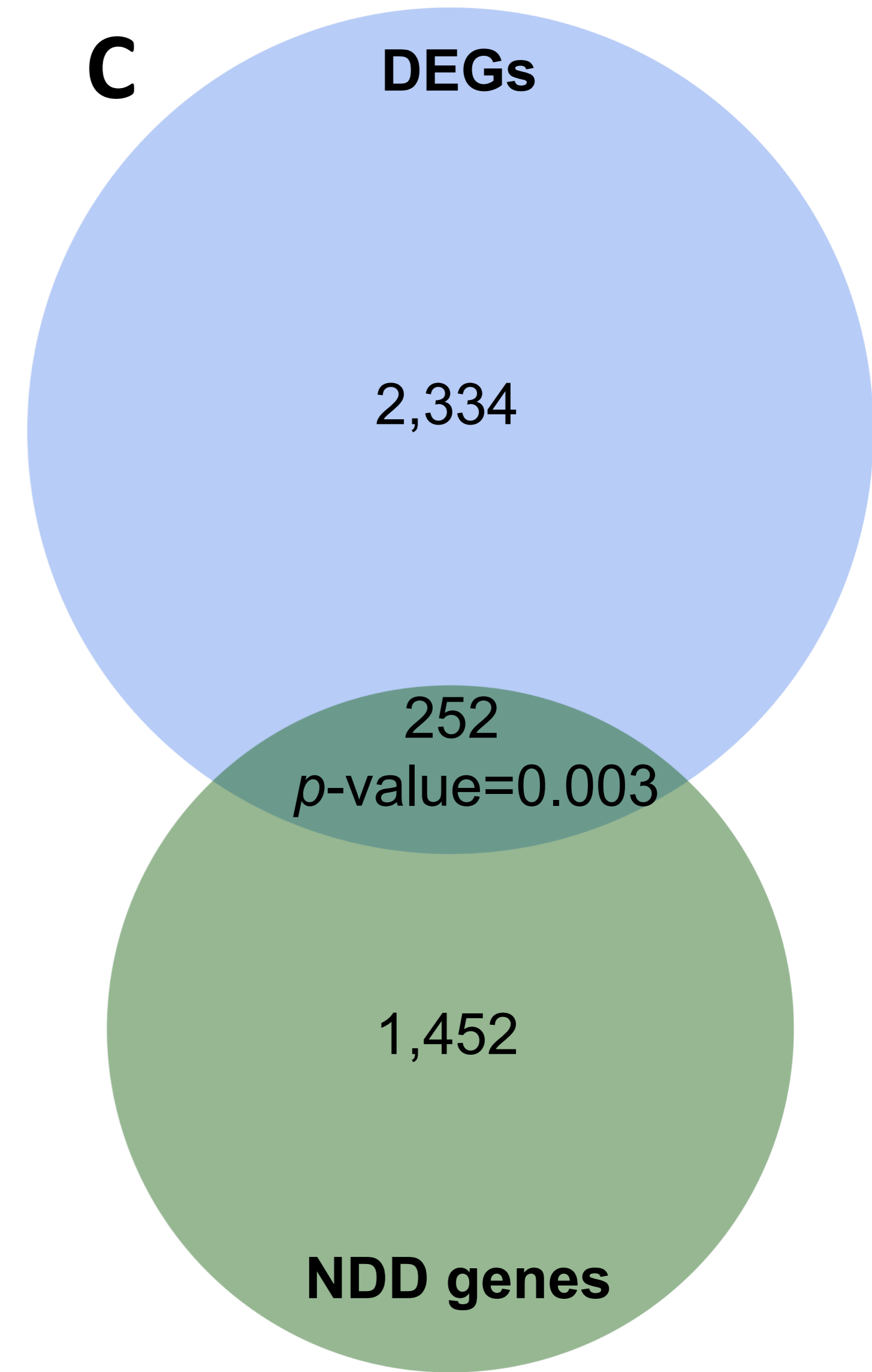
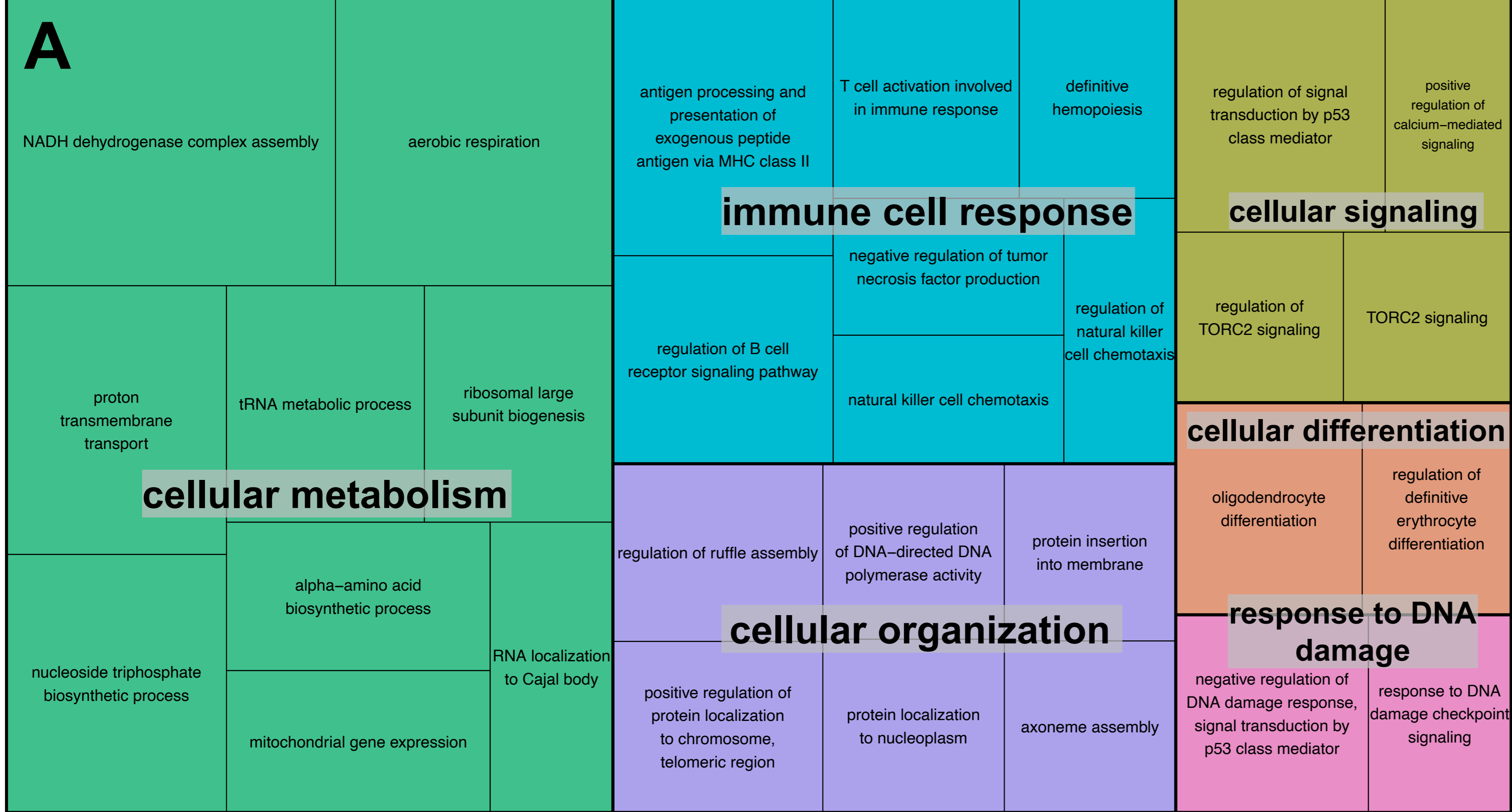
509 **Table 1.** Enriched overrepresented GO terms in DEGs of 15q13.3 individuals. FWER:  
510 family-wise error rate corrected  $p$ -value; #genes: number of DEGs involved in the function.  
511 For genes included in the nodes refer to Supplementary Table S2.

GO ID	Ontology	GO term	raw $p$ -value	FWER	#genes
GO:0007399	biological process	nervous system development	1.93E-05	0.036	32
GO:0003677	molecular function	DNA binding	0.0001	0.046	183

512

513

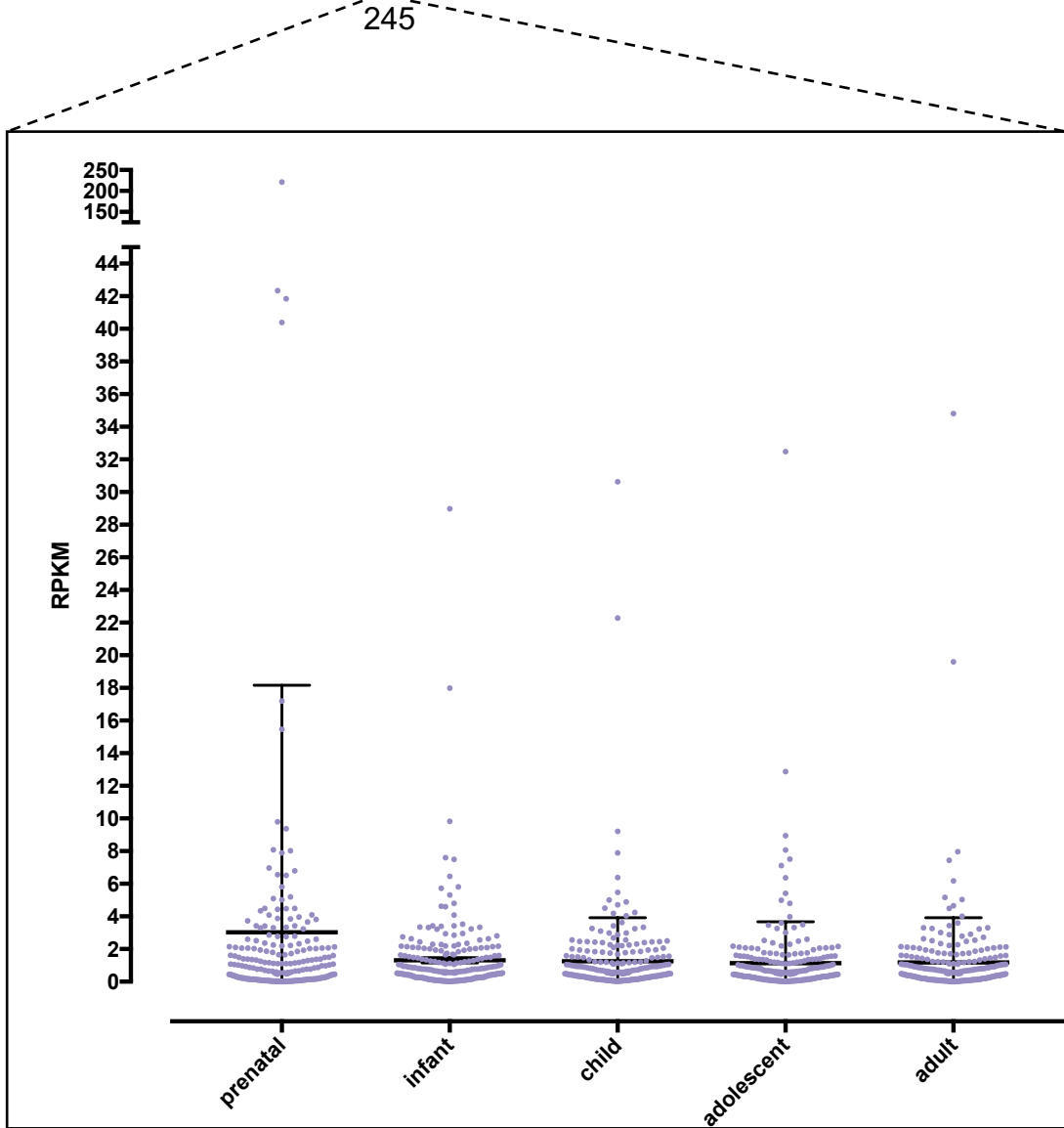
**A****B**

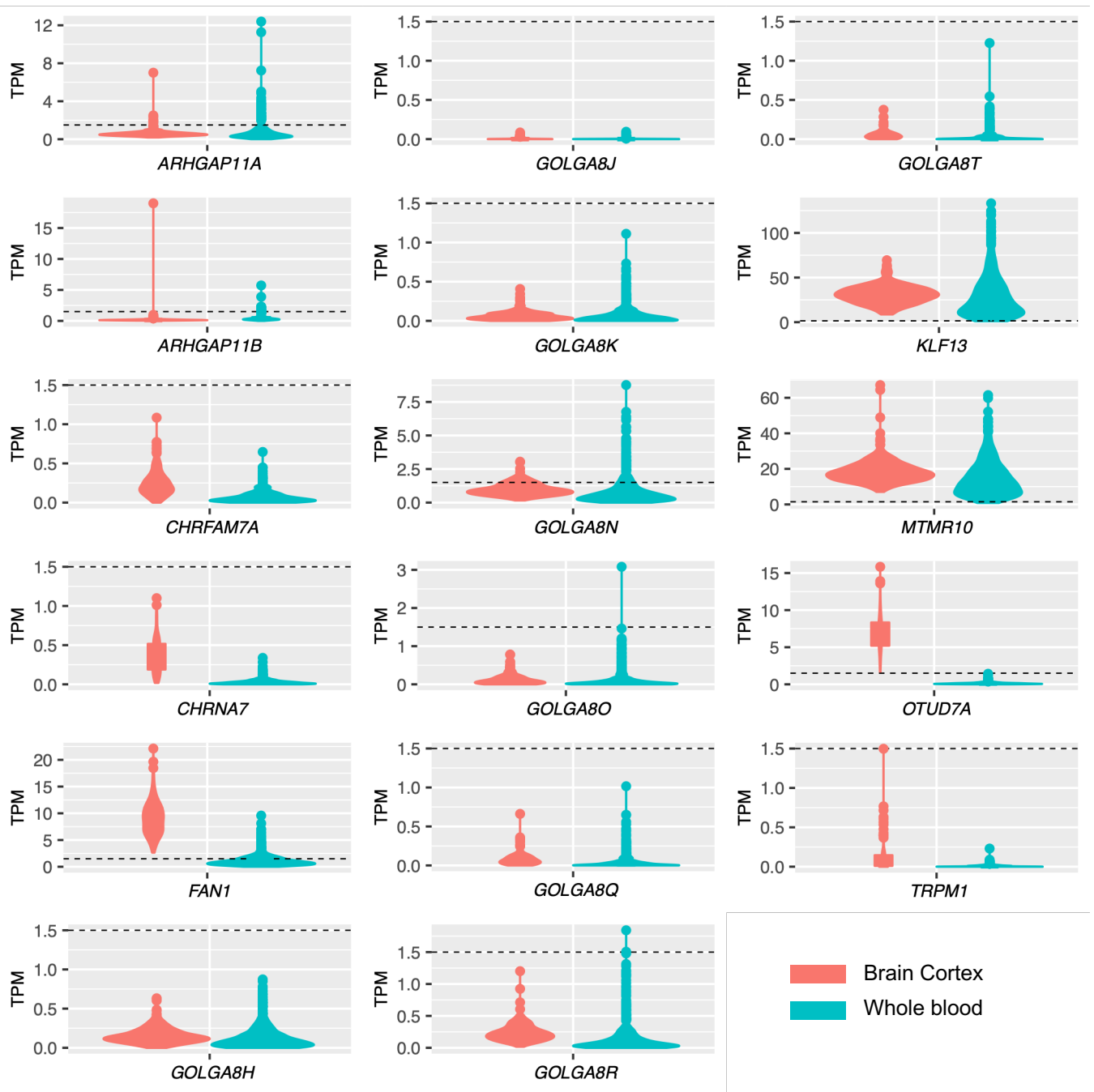


Total=2,334 DEGs



- DEGs with brain cortex expression
- DEGs not expressed in brain cortex, with expression levels in Allen Brain Atlas
- DEGs not expressed in brain cortex, nor in Allen Brain Atlas





**Supplementary Fig. S1.** Expression levels of genes located in the 15q13.3 microdeletion region. TPM (transcript per kilobase million mapped reads) values of gene expression levels are depicted for brain cortex tissue and whole blood. The dashed lines represent 1.5 TPM. Expression values were obtained from PTEE (<https://bioinf.eva.mpg.de/PTEE/>).